



Hourly land-use regression models based on low-cost PM monitor data

Mauro Masiol^{a,b}, Naděžda Zíková^{b,c}, David C. Chalupa^d, David Q. Rich^a, Andrea R. Ferro^e, Philip K. Hopke^{a,b,*}

^a Department of Public Health Sciences, University of Rochester Medical Center, Rochester, NY, USA

^b Center for Air Resources Engineering and Science, Clarkson University, Potsdam, NY, USA

^c Institute for Environmental Studies, Faculty of Science, Charles University, Prague, Czech Republic

^d Department of Environmental Medicine, University of Rochester Medical Center, Rochester, NY, USA

^e Department of Civil and Environmental Engineering, Clarkson University, Potsdam, NY, USA

ARTICLE INFO

Keywords:

Exposure assessment

Land-use regression

Low-cost monitors

PM_{2.5}

ABSTRACT

Land-use regression (LUR) models provide location and time specific estimates of exposure to air pollution and thereby improve the sensitivity of health effects models. However, they require pollutant concentrations at multiple locations along with land-use variables. Often, monitoring is performed over short durations using mobile monitoring with research-grade instruments. Low-cost PM monitors provide an alternative approach that increases the spatial and temporal resolution of the air quality data. LUR models were developed to predict hourly PM concentrations across a metropolitan area using PM concentrations measured simultaneously at multiple locations with low-cost monitors. Monitors were placed at 23 sites during the 2015/16 heating season. Monitors were externally calibrated using co-located measurements including a reference instrument (GRIMM particle spectrometer). LUR models for each hour of the day and weekdays/weekend days were developed using the deletion/substitution/addition algorithm. Coefficients of determination for hourly PM predictions ranged from 0.66 and 0.76 (average 0.7). The hourly-resolved LUR model results will be used in epidemiological studies to examine if and how quickly, increases in ambient PM concentrations trigger adverse health events by reducing the exposure misclassification that arises from using less time resolved exposure estimates.

1. Introduction

Exposure to increased mass concentrations of airborne particulate matter (PM) has been associated with multiple adverse health effects (Pope et al., 2009; Anderson et al., 2012; Raaschou-Nielsen et al., 2013; Loomis et al., 2013; Dadvand et al., 2013). In the United States, criteria air pollutants, including PM₁₀ and PM_{2.5}, are measured at fixed air quality monitoring stations in the National Ambient Air Quality Standards (NAAQS) compliance monitoring network managed by state, local, or tribal agencies (Solomon et al., 2014). Generally, one or at most, a few urban stations are deployed within major cities to assess the citywide concentrations of air pollutants for regulatory compliance purposes. The resulting data are also commonly used to estimate the exposure for the residing population. However, air pollution can exhibit spatial variability within urban areas (Hodzic et al., 2005; Isakov et al., 2007; Levy and Hanna, 2011; Eeftens et al., 2012; Hoek et al., 2015; Shairsingh et al., 2018) because of the locations and strengths of local sources, the effect of street canyons and complex terrain, and urban heat island effects. The spatial coverage of routine monitoring networks

is generally insufficient to capture this spatial variability required to accurately represent human exposure for use in epidemiological studies without some degree of exposure misclassification. Such limited accuracy may negatively bias health effects model estimates and underestimate the air pollution impacts on human health (Thurston et al., 2009; Sarnat et al., 2010; Özkaynak et al., 2013).

Recent studies have reported increased mortality associated with increased PM_{2.5} concentrations in the previous few hours (Lin et al., 2017a, 2017b). Given the temporal and spatial variability in PM_{2.5} concentrations, it is important to obtain sufficient temporal and spatial resolution in the PM exposures to provide adequate information for epidemiological studies to estimate its short-term health impacts. Land-use regression (LUR) models (Hoek et al., 2008, 2011; Clougherty et al., 2008, 2013; Beelen et al., 2010; Hoogh et al., 2013) incorporate monitoring data and land-use variables to provide improved exposure estimates. Previously, a daily model was developed to provide estimates of the wood smoke tracer (Su et al., 2015a), Delta-C, and black carbon (BC) concentrations at the residences of 246 ST-elevation myocardial infarction (STEMI) patients treated at the University of Rochester

* Corresponding author at: Department of Public Health Sciences, University of Rochester Medical Center, Rochester, NY, USA.
E-mail address: phopke@clarkson.edu (P.K. Hopke).

Medical Center during the winters of 2008–2012. Using case-crossover methods, the rate of STEMI was associated with increased Delta-C and BC concentrations on the same and previous 3 days after adjusting for 3-day mean temperature and relative humidity (Rich et al., 2018). Since this LUR model only provided 24-h exposure estimates, this study could not examine whether increased pollutant concentrations in the previous few hours were associated with an increased rate of STEMI. Thus, it could not fully assess the role of these particulate species in triggering STEMI since prior work had found that recent short-term exposures were associated with STEMI events (Gardner et al., 2014; Pope et al., 2015; Zhang et al., 2016; Argacha et al., 2016; Akbarzadeh et al., 2018). Therefore, sophisticated spatial-temporal models are needed to minimize exposure error and bias by better predicting concentrations at individual locations for individual hours, especially for outcomes with short-term responses to air pollution (i.e., < 24 h).

Recent development of low-cost PM monitors (LCMs) permits the cost-effective deployment of many sampling points. LCMs are becoming valuable by enabling the increased spatial resolution of air quality measurements (Snyder et al., 2013; Kumar et al., 2015; Holstius et al., 2014). LCMs are much less expensive than scientific-grade instruments, physically smaller and lighter, and have low power demands. However, they are not designed to meet rigid performance standards and require careful calibration and post-processing of data (Budde et al., 2013; Kumar et al., 2015; Holstius et al., 2014; Wang et al., 2015; Gozzi et al., 2016; Sousan et al., 2016; Manikonda et al., 2016; Carminati et al., 2017; Zikova et al., 2017a, 2017b; Kelly et al., 2017).

Even with many LCMs providing substantially improved spatial resolution and temporal detail, they cannot provide detailed personal exposure estimates at any given location and time. Thus, models are needed to predict concentrations when and where there are no monitoring data. LUR models incorporate multiple kinds of predictor variables. These predictors may include highway locations, traffic volumes, population data, property assessment information, land-use, physical geography, and meteorology (Hoek et al., 2011, 2015). Linear regression models are then developed to determine which predictors (independent variables) best reproduce the monitoring data (dependent variable).

Rochester is a medium-sized city in the northeastern U.S. Previous studies (Su et al., 2015a) performed mobile measurements throughout the urban area of Rochester by deploying scientific-grade instruments for black carbon (2-wavelength aethalometer) and PM_{2.5} (beta attenuation monitors). The data were then used to feed LUR models. However, the PM results showed poor fits to the data ($R^2 \sim 0.35$), and therefore, only black carbon results were presented. Thus, the prior work evinced large spatial variations in PM across the urban area. Rochester has only a single site at which pollutants are measured using EPA Federal Reference (FRM) or Federal Equivalent (FEM) Methods. Thus, the intraurban spatial variability of PM cannot be estimated using a single central site given that the nearest air quality monitoring site is located 60 miles away in Buffalo, NY. Alternative approaches are needed to improve the spatial coverage and reduce misclassification in personal exposures and allow effective study of the health effects of ambient air pollutants.

This study assesses the hourly small-scale variability of PM across Rochester by using data collected with LCMs during a winter campaign as input for LUR models. The study takes advantage of the synergy between an extensive set of spatially resolved PM data and the application of sophisticated LUR models based on the deletion/substitution/addition (D/S/A) algorithm (Sinisi and van der Laan, 2004a, 2004b). Model robustness and reliability is insured by a cross-validation scheme and incremental F-test statistic is used to select the optimal number of predictors to be included into the models. The exposure estimates from these models will be used in future studies of PM impacts on STEMIs and other short-term health outcomes.

2. Materials and methods

2.1. Study area

The study was performed in Monroe County, New York, U.S., which lies on the southern shore of Lake Ontario and includes the City of Rochester (~210,000 inhabitants, 2010 Census). Monroe County is the center of the greater Rochester metropolitan area (~1.1 million inhabitants), which also encompasses several surrounding counties (Supplementary Information (S) Fig. S1). The emission scenario comprises typical diffuse urban emissions and few industrial sources. Road traffic is a major emission source across the metropolitan area on highways and secondary roads (Fig. S1). Natural gas and bottled liquid petroleum gas (LPG) are largely used for domestic and commercial heating. However, residential wood combustion is becoming an increasingly used alternative for space heating (NYSERDA, 2015). Biomass burning has recently been estimated to contribute up to ~30% of PM_{2.5} mass in winter in this area (Wang et al., 2011, 2012). Industrial emissions are dominated by a coal-fired cogeneration plant located in the suburban area (Fig. S1); off-road transport (diesel rail, shipping, airport) and wastewater treatment plants are other potential local PM sources. Regional advection of polluted air masses from Toronto (ON), Buffalo (NY), the Ohio River Valley, and the eastern coast of U.S may also affect the air quality in this region (Emami et al., 2018).

2.2. Experimental

Ambient PM concentrations were measured using commercially available LCMs (Speck, Airviz Inc., Pittsburgh, PA, USA) during the heating seasons of 2015/2016 (December to March) and 2016/2017 (November to March) at 23 and 25 residential locations, respectively. These monitors are described in detail by Manikonda et al. (2016). This system uses an infrared LED-based Samyoung DSM501A dust sensor. A small fan pulls the air into the sensor and the concentrations can be measured with an adjustable time resolution (30 s to 4 min). Data are stored in the internal memory or uploaded to the manufacturer's server when connected to a Wi-Fi network. Preliminary tests reported stable responses over wide ranges of particle concentrations (0–1000 µg/m³) and high repeatability of results (Wang et al., 2015). Lab tests showed these units have a good agreement with conventional scientific-grade instruments (aerodynamic particle sizer and GRIMM spectrometers) when exposed to wide concentration ranges (0–500 µg/m³) of both cigarette smoke and test dust particles (Manikonda et al., 2016). Field studies reported large biases, but good reproducibility and an overall precision of $12.2 \pm 6.2\%$ when measuring outdoor PM concentrations (Zikova et al., 2017a). Zikova et al. (2017b) presented the data collected over two winter campaigns and indicated that the use of a network of monitors can be useful to estimate the spatial and temporal variability of urban PM.

The LCMs were placed outdoors at the homes (mostly in backyards) of volunteers having wood burning appliances in their homes or reporting frequent wood smoke in their neighborhood. An additional LCM was placed at the New York State Department of Environmental Conservation monitoring site in Rochester, NY (USEPA site code 36-055-1007; 43°08'46"N, 77°32'52"W). Fig. S2 presents the spatial characteristics of the sampling sites during the 2015/2016 season in terms of the percent coverage of natural and anthropogenic land cover categories and road types calculated with 250 m buffers around each site. Fig. S2 shows that the sites were broadly representative of both natural and anthropogenic environments, i.e. all the land cover categories included into the LUR models were generally represented by the selected sites. Results for the road characteristics show that 2 sites were close to highways, 8 sites were located near major roads and all sites reported ~2% to ~16% of the buffer area represented by local roads.

The LCMs were mounted in waterproof plastic-fiberglass boxes with two 90° bent inlets (2 cm in diameter) for air exchange and a 6 W bulb

to prevent freezing (Fig. S3). The internal fan in the unit was used to induce flow into the box. PM concentrations were recorded every minute. A mid-term check of the sampling sites was performed to check and maintain the instruments, clean the box and the inlets and outlets.

2.3. Data handling

A known limitation of LCMs is their low accuracy (US EPA, 2017). However, they do possess reasonable precision (Manikonda et al., 2016). Thus, the data from such sensors can be made useful through appropriate calibration techniques (Budde et al., 2013, 2014; Holstius et al., 2014; Manikonda et al., 2016; Zikova et al., 2017a, 2017b; Kelly et al., 2017; Li et al., 2014). Data were processed as previously described (Zikova et al., 2017a, 2017b) providing a robust dataset with 1-h time resolution. Hourly averages were computed from the original 1 min time-resolved data when at least 75% of records (45 min) were available for a given hour. Instrumental biases were determined for each monitor using the results of a 3-day field co-location period with a GRIMM 1.109 aerosol spectrometer. Separate corrections were applied to the data from each monitor by multiplying by the ratios between mean PM_{2.5} concentration measured by the GRIMM and those measured by the individual LCMs (Zikova et al., 2017a, 2017b). No detection limits (DL) were set for the Specks.

2.4. Air quality and spatial predictor variables

The variables available for the LUR modeling are listed in Table 1. Two variable types were incorporated into the models. One class of variables are specific to each given location in the modeling domain

and do not change over time. They include:

- **Housing.** The number (*N*) of bedrooms, fireplaces, kitchens, and stories, property value, and year built were obtained from the property assessment data of Monroe County for 2013. For each parcel, *N* was calculated as (parcel count/parcel area in ha)/100. The data were rasterized at 10 × 10 m spatial resolution, and predictors were calculated as sum of values within each buffer.
- **Roadways.** The geocoded locations of highway, major, and local roadways were computed using road network data provided by ESRI Business Analyst 2010 (Redlands, CA, USA). The data were rasterized (10 × 10 m) and the percent of covered areas was calculated for each buffer;
- **Railroad.** The geocoded location of railroad lines was obtained from NYS Department of Transportation (NY DoT) and handled similarly to roadways;
- **Traffic Counts.** The annual average vehicular daily traffic counts (AADT) for highway and major roads were obtained from the NY DoT highway performance management system (HPMS). AADT data are expressed as annual averages and the hourly variations are not accounted for. The diurnal traffic profiles for typical major roads in Rochester during winter were separately provided by DoT, which commissioned hourly counts of traffic during two whole weeks (December and January). The traffic profiles are shown in Fig. S4. The combined hour of day and day of week average profiles were then used as a scaling factor to model the AADT over the study period (called “modeled AADT”). Holidays were modeled as Sundays. AADT and modeled AADT were both included in the predictor list after data were rasterized at 10 × 10 m spatial resolution and

Table 1
List of variables available for development of the land use regression models.

| Variable name | Source of information | Buffer/not buffer |
|----------------------------|--|-------------------|
| Bedrooms | Property assessment data of Monroe County | Buffer |
| Fireplaces | Property assessment data of Monroe County | Buffer |
| Kitchens | Property assessment data of Monroe County | Buffer |
| Stories | Property assessment data of Monroe County | Buffer |
| Property value | Property assessment data of Monroe County | Buffer |
| Year built | Property assessment data of Monroe County | Buffer |
| Highways | NYS Department of Transportation | Buffer |
| Major roads | NYS Department of Transportation | Buffer |
| Local roads | NYS Department of Transportation | Buffer |
| AADT | NYS Department of Transportation | Buffer |
| Modeled AADT | NYS Department of Transportation | Buffer |
| Railways | NYS Department of Transportation | Buffer |
| DEM | USGS | Buffer |
| NLCD11-Water | USGS National Land Cover Database (NLCD) | Buffer |
| NLCD21-Open space | USGS National Land Cover Database (NLCD) | Buffer |
| NLCD22 + 23-Develop. areas | USGS National Land Cover Database (NLCD) | Buffer |
| NLCD24-High develop. | USGS National Land Cover Database (NLCD) | Buffer |
| NLCD31-Barren lands | USGS National Land Cover Database (NLCD) | Buffer |
| NLCD40s-Forests | USGS National Land Cover Database (NLCD) | Buffer |
| NLCDs50s-Scrubs | USGS National Land Cover Database (NLCD) | Buffer |
| NLCD70s-Herbaceous | USGS National Land Cover Database (NLCD) | Buffer |
| NLCD81-Pasture/hay | USGS National Land Cover Database (NLCD) | Buffer |
| NLCD82-Cultivated | USGS National Land Cover Database (NLCD) | Buffer |
| Hourly traffic profile | NYS Department of Transportation | Not buffer |
| CO | NYS Department of Environmental Conservation | Not buffer |
| NO | NYS Department of Environmental Conservation | Not buffer |
| NO ₂ | NYS Department of Environmental Conservation | Not buffer |
| NO _y | NYS Department of Environmental Conservation | Not buffer |
| SO ₂ | NYS Department of Environmental Conservation | Not buffer |
| O ₃ | NYS Department of Environmental Conservation | Not buffer |
| TEOM PM _{2.5} | NYS Department of Environmental Conservation | Not buffer |
| BC | NYS Department of Environmental Conservation | Not buffer |
| Delta-C | NYS Department of Environmental Conservation | Not buffer |
| Air temperature | Greater Rochester International Airport | Not buffer |
| Humidity | Greater Rochester International Airport | Not buffer |
| Pressure | Greater Rochester International Airport | Not buffer |
| Wind <i>u</i> | Greater Rochester International Airport | Not buffer |
| Wind <i>v</i> | Greater Rochester International Airport | Not buffer |

sum of values within each buffer was calculated.

- **Elevation.** The digital elevation model (DEM, 10×10 m) was obtained from the U.S. Geological Survey (USGS) and the average elevation was set as buffer statistics.
- **Land-use.** Land-use data were extracted from the USGS National Land Cover Database (NLCD) for 2011 (30×30 m resolution) including single and composed classes: open water (category no. 11), open space (21), developed low and medium (22 + 23) and high (24) intensity, barren lands (31), forests (41 + 42 + 43), scrublands (51 + 52), herbaceous (71 + 72), pasture/hay (81) and cultivated crops (82).
These variables provide average values within circular buffers drawn around each sampling location with increasing radii from 50 m to 5000 m at 50 m steps (total 100 buffers for each site). Buffer statistics were calculated for each buffer size and predictor variable. The other variables are general to the area and change from hour-to-hour. These measured variables include:
- **Meteorology.** Since meteorology may further affect the PM concentration some weather variables measured at the Rochester international airport (KROC) were also added, including air temperature, humidity, barometric pressure and scalar components of wind (u , v relative to the North-South and West-East axes, respectively). Weather data collected at KROC were taken as representative of the meteorology across the County (Wang et al., 2011; Emami et al., 2018).
- **Air Quality Data.** Because PM concentrations can be correlated to other air pollutants, hourly air quality data measured at the DEC site were also included into the model as independent variables. CO, NO, reactive nitrogen (NO_y), SO_2 , O_3 , $\text{PM}_{2.5}$ (TEOM-FDMS) were measured using FRM or FEM methods (details provided in Table S1). Nitrogen dioxide was assessed as the difference between NO_y and NO. Hourly concentrations of BC and Delta-C (marker for biomass burning calculated as difference between absorbance at 370 and 880 nm; Wang et al., 2011) were also measured with a 2-wavelength aethalometer. Raw data were corrected for non-linear loading effects (Turner et al., 2007; Virkkula et al., 2007). All of the air pollution data collected by DEC that were below the DLs were set to DLs/2 (Table S1).

2.5. D/S/A model

A comprehensive discussion of the D/S/A algorithm has been provided by Sinisi and van der Laan (2004a, 2004b) This algorithm has been successfully applied in several prior LUR model developments (Beckerman et al., 2013a, 2013b; Su et al., 2015a). Briefly, the D/S/A approach implements a data-adaptive estimation method from which estimator selection is based on cross-validation under specified constraints. The D/S/A interactively generates n -order polynomial generalized linear models in three steps: (i) a deletion step removing a term from the model; (ii) a substitution step replacing one term with another; and (iii) an addition step adding a term to the model. The cross-validation scheme (V -fold) randomly partitions the original input dataset into V equal size subsamples ($V=3$, in this study): $V-1$ subsamples are used as training dataset and the remaining subsample is retained as the validation data for testing the model. The V -fold process minimizes the chance of overfitting the model because the data validation is repeated V times (i.e. all V subsamples are used once as validation dataset) and results are combined to produce a final estimation. The D/S/A models were run under R (version 2.15.3).

3. Results and discussion

3.1. Overview of LCM calibration and data

The average (\pm standard deviation) $\text{PM}_{2.5}$ concentrations measured by the TEOM-FDMS (FEM method) at the DEC site were 8.0 ± 5.6

(range $1\text{--}41 \mu\text{g}/\text{m}^3$) and $6.0 \pm 4.7 \mu\text{g}/\text{m}^3$ (range $1\text{--}32 \mu\text{g}/\text{m}^3$), respectively in 2015/2016 and 2016/2017. The mean concentration during the second period averaged only 74% of the first period mean concentration. After the correction of the LCMs using the results of the co-location with the GRIMM spectrometer, a similar decrease in concentrations for the second year was also observed by the LCMs (71%). However, the corrected concentrations measured by the LCMs (average 3.5 ± 0.9 and $2.4 \pm 0.4 \mu\text{g}/\text{m}^3$ during the first and second campaign, respectively) were lower than the FEM values.

The underestimation suggests that the bias correction did not adequately reflect the differences between the TEOM-FDMS and the GRIMM values (Halliburton et al., 2007). A further correction based on the TEOM-FDMS data was performed by multiplying the LCM PM by the mean ratios of the TEOM/LCM PM values recorded in each of the two seasons. This scaling factor provided “FEM-like” average $\text{PM}_{2.5}$ concentrations. The correlation between TEOM $\text{PM}_{2.5}$ and LCM PM at the DEC site (r) was 0.47 across all hours of the day during the 1st season, but the r was only 0.1 during the 2nd season. The correlations among the LCMs were also substantially higher during the first season (Zikova et al., 2017b). The potential degradation of the sensing elements was not substantial since the LCM results agreed with the GRIMM ($r = 0.6$) during the co-location test after the second sampling campaign. It is likely that the low $\text{PM}_{2.5}$ concentrations observed during the 2nd season reduced the signal-to-noise ratio in the data. Thus, the result suggest that the concentrations are sufficiently low that the responses from the LCMs that the 2nd season results were unreliable and unusable to develop the LUR models. Consequently, the LUR models were based only on the 1st season data.

Despite these limitations, a preliminary analysis of PM data for the first season showed reasonable sit-to-site correlations (Fig. S5). The correlations between the TEOM and the LCM deployed at DEC site ranged from 0.4 (6 A.M.) and 0.6 (evening, midnight). The different PM sources (traffic, heating) and atmospheric chemical processing during the day may drive the agreement among the instruments (LCMs detect particles primarily in the size range of $0.5\text{--}3 \mu\text{m}$). In addition, the LCM network data were also able to produce sensible daily spatial patterns (Zikova et al., 2017b). Maps of interpolated PM concentrations were computed for each hour of the day. Results show minimal concentrations over all the sites at 5–6 A.M., followed by an increase until noon at several sites due to the morning rush hour. Then, the PM concentrations were almost stable until about 3 P.M., when a second peak occurs and raises the PM concentration to maximum levels (around 6 P.M., i.e., during the evening rush hour). These maps are available as animations at <http://www.mdpi.com/1424-8220/17/8/1922/s2>.

3.2. Relationships between PM and predictors

The relationships between the dependent variable (LCM PM) and each independent variable (both buffer and non-buffer predictors) were initially investigated by calculating the Pearson correlation coefficients. Figs. S6 and S7 show the correlations with the air pollutants measured at the NYS DEC site and the airport weather variables for each weekday and weekend day hour, respectively. Generally, data collected on weekdays showed the highest positive correlations with CO, NO_y , SO_2 , $\text{PM}_{2.5}$, BC, and Delta-C. Lower correlations were found for weekend days, irrespective of the sampling season (Fig. S6). The correlations with nitrogen oxides and BC exhibited peaks during the morning rush hours (7–10 A.M.), evening rush hours (4–10 P.M.), and overnight. This pattern may be due to higher traffic emissions during the rush hours on weekdays. Lower mixing layer heights and wind speeds may contribute to the nighttime correlations. Low correlations were found with the measured weather variables (Fig. S7). The uniformly low correlations with RH ($r < |0.27|$) indicates a limited effect of atmospheric humidity on the LCM measurements since hygroscopic growth is a known issue for light scattering systems (Lundgren and Cooper, 1969; Covert et al., 1975; Wang et al., 2015; Zikova et al., 2017a).

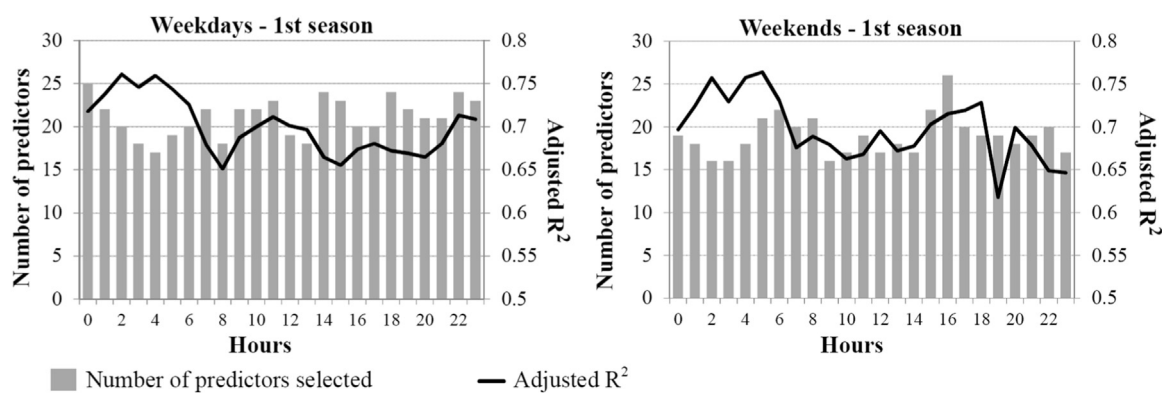


Fig. 1. Results of the linear models for the weekdays (left) and weekends/holidays (right).

Fig. S8a-d present the distance decay curves for all the buffer predictors: such curves express the correlation of the dependent variable against the predictor statistics at varying buffer sizes and hours, separately for weekdays and weekends. Generally, the distance decay curves of spatial predictors show: (i) correlations ranging from -0.35 – 0.4 ; (ii) similar hourly patterns for increasing buffer radii for most predictors; (iii) similar patterns during weekdays and weekends; and (iv) rapid variations of the correlations by varying the buffer radii for some predictors.

3.3. Model set-up

The final dataset included $\sim 55,000$ observations (hourly PM concentrations at the sites during the 2015/2016 season). There were 2297 possible spatial variables, including 23 predictors for each buffer size with 23,000 possible buffers after excluding the null variance buffers. Such buffers occurred for some predictors at the smaller buffer sizes. There were 9 measured air pollutants, 5 weather variables and the estimated hourly traffic counts. The cross-validation scheme was set such that each model run used 2/3 of observations for model training and 1/3 for model validation. Final models were built and tested after evaluating numerous preliminary trials using different model set-ups, data sets, and sets of predictors:

- Models were originally run for each hour, irrespective of the day of week. However, road traffic is a major local source of PM and exhibits different hourly profiles during weekdays and weekends (Fig. S4). Final models were therefore run separately for weekdays (Monday to Friday) and weekends (Saturday and Sunday, and holidays falling on weekdays), improving the fit with the measured PM concentrations.
- Distance decay curves for several buffer predictors (Fig. S8a-d) show relatively high correlations even for larger buffers. Since previous studies reported distances of up to 5 km for impacts on $PM_{2.5}$ (Beckerman et al., 2013a), and PM-bound components (Su et al., 2015b), all buffers were included in the models. These large buffers may be associated with background effects. The distance decay curves were also computed using square root and quadratic predictors. No improvement of correlations have been detected with transformed data.
- Previous applications of the D/S/A model to the LUR problem (Beckerman et al., 2013a) used log-transformed data to decrease the likely violation of the assumption of homoscedastic errors. However, using transformed data may produce results that are difficult to interpret and initial data assessments, distance decay curves were examined for log transformed and square root value and found no improvement in the calculated correlations. Thus, based on these results and the prior experience (Su et al., 2015a, 2015b), we did not apply any data transformations.

- Since the number of independent variables selected by the model is a user-specified constraint, the optimal number of variables was subsequently selected by analyzing the statistical significance using incremental (partial) F-tests. The model was run sequentially with the addition of a term (from 6 to 50 variables) until no statistically significant ($p < 0.05$) increase in adjusted R^2 were obtained.
- D/S/A implements an aggressive covariate search algorithm to fit generalized linear models predicated on the power of cross-validation (CV) to select the best predictive models. This CV method has asymptotically optimal properties for deriving and assessing performance of predictive models (an exhaustive explanation is provided in Beckerman et al. (2013a, 2013b) and references therein). Briefly, the cross-validation performance is estimated using the L2 loss function (called CV risk). The CV risk is defined as the expectation of the squared cross-validated error and is based on the CV- R^2 values. The approach tests nearly all covariate combinations. Then, the selection of the best model implemented into the D/S/A algorithm is based on a plot that shows the average CV risk as a function of the size of the model. Generally, as the model increases in size, the CV risk decreases until it reach a minimum. In this study, the best models were selected following the F-test results, which also returned low CV risks (close to minima).
- Both first and mixed first- and second-order polynomial function models were computed as discussed elsewhere (Su et al., 2015a, 2015b). First order (linear) models were ultimately selected as the best solutions because they generally required a lower number of predictors to meet the incremental F-test criteria (parsimony). In addition, using second-order polynomial functions may produce solutions including both linear and squared terms with opposite signs for the same predictor. This situation should be avoided because (i) the interpretation of results is complicated and (ii) the models show very limited improvement (Su et al., 2015a). Fig. S9 shows an example of the application of incremental F-test.

3.4. Model results

The diagnostics (adjusted R^2 and number of selected predictors) for the selected linear models are summarized in Fig. 1. The list and the occurrence of predictors are reported in Fig. 2 and Fig. S10 for weekdays and weekends, respectively. Models selected 17–25 predictors (average 21) during weekday hours, with adjusted R^2 ranging between 0.66 and 0.76 (average 0.7) (Fig. 1, left plot). Weekend models included 16–26 predictors (average 19) with R^2 in the 0.63–0.77 range (average 0.7) (Fig. 1, right plot). A decrease in R^2 values occurred between 7 and 9 A.M., i.e. morning rush hours, and higher R^2 values were found overnight (2–4 A.M.). High traffic emissions may produce compositional changes that result in poorer agreement among the monitors. Fresh emitted carbonaceous particles are emitted during rush hours resulting in changes in the particle scattering and, possible biases in the

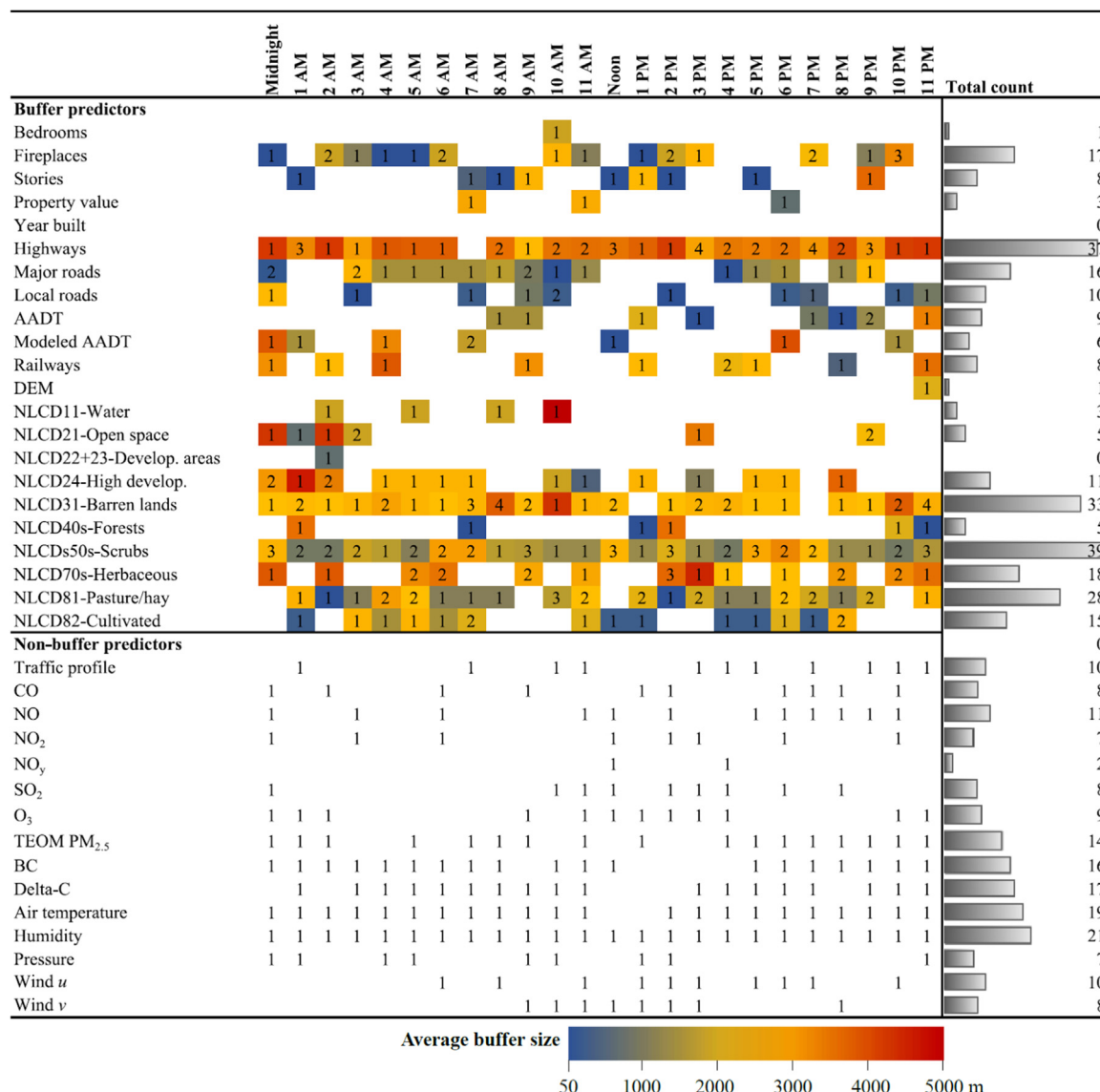


Fig. 2. Model results for weekdays in the 1st season data. For each predictor selected by the model, the colors (see bottom legend bar) report the buffer size, while the numbers refer to the times a predictor is called during a hour (in case of buffer predictors called more than one time, the color refers to the average of the buffers). The right bar plots on the right are proportional to the total count, i.e. the number of times a predictor is called overall the 24 h, irrespective of the buffer size.

reported mass although such effects should have been modeled by the BC variables measured at the central site. Hourly traffic profiles included in the models (Fig. S4) were previously measured but were not routinely monitored by DoT on several main roads. The hourly traffic patterns on local roads were estimated. Generally, highways, scrublands, barren lands and pasture/hay dominated the occurrence of buffer predictors, with highways showing the highest buffer sizes (often greater than 2 km), followed by barren lands (Fig. 2 and S10). Local roads involved smaller buffer sizes (≤ 800 m).

The effect of road traffic on the spatial variability of PM is evident. Traffic-related predictors were selected for all hours, with highways affecting the PM concentrations at greater distances, local road on small scales, and major roads at an intermediate level. The effect of highways was significantly lower during the weekends than during weekdays. Humidity and air temperature were the most commonly selected weather variables. DC, BC, and PM_{2.5} were the more frequently included air pollutants. This latter result further indicates the role of carbonaceous including traffic exhaust and wood smoke affecting the PM concentrations detected by the light scattering-based LCMs.

To illustrate the model output, PM concentrations were estimated

for midnight and noon on a typical weekday and a typical weekend day. These results are shown as a set of maps in Fig. S11. These days were selected because the measured DEC air pollutants concentrations and weather parameters approximated the whole season mean values (no pollution peaks, clean air events, nor extreme weather conditions). The maps were computed by calculating the buffer statistics at a 250×250 m grid resolution. The maps show reasonable spatial patterns. Higher concentrations were modeled within the downtown Rochester area, except during weekday at noon. This result reflects higher emission rates from domestic heating occurring overnight and during the weekends overall the day, while less domestic emissions are expected on working days at noon (people at work). The effect of road traffic over the major roads is mostly evident on weekdays at midnight (highways and major roads) and on weekends at noon (local and major roads). These results may be driven by (i) the combined effect of the lower mixing layer height overnight and traffic emissions in the evening hours, and (ii) the traffic peak observed around noon on the weekends that is not present on weekdays (Fig. S4). The absence of a clear spatial pattern on weekdays at noon is likely related to the greater pollutant dispersion by higher mixing layer height, higher wind speeds, and the

lower downtown traffic volumes around noon on workdays. These results provide confidence in the ability of these models to extrapolate exposure assessments in other periods to support future epidemiological studies.

3.5. Final remarks, limitations, and future needs for research

Urban central air quality monitoring sites are located to represent the citywide air quality and are usually used to assess the community exposure to air pollutants. However, the sparse spatial coverage of current air quality networks is likely insufficient to adequately capture the intraurban variability in PM concentrations. This spatial variation can be determined using special sampling campaigns performed by coupling data measured with scientific-grade instruments and subsequent LUR modeling. However, extended campaigns using scientific-grade instruments are difficult to perform due to high costs, power requirements, logistics, and maintenance needs. In addition, although these studies provide precise and accurate data, they usually only allow for a limited numbers of locations, short duration monitoring periods and/or measurements that may not produce a full set of 24/7 data. Consequently, these methods still lack the spatial resolution and temporal coverage needed for accurate exposure assessments. Mobile monitoring will have mismatched space-time pairings and limited temporal data. This latter issue is critical when the investigated air pollutant is affected by strong diurnal/weekly patterns.

The combined use of a network of LCMs and LUR modeling provide an effective way to estimate the intraurban PM variability. This study does not provide a direct evidence that the LCM-LUR approach is preferable to using a reference grade central monitor. To answer that question directly would require a double sampling campaign with LCMs and conventional research-grade instruments collocated side-by-side. Such a study would be costly and difficult to justify and execute. The results presented here are promising and show that LCM-LUR is a viable way that can be further developed. Data provided by the LCMs are able to catch the intra-urban spatial variability of PM although affected by measureable and correctable bias. The subsequent application of LUR has the potential advantage of extending the results to other times and locations and better modeling the spatial variability of PM with reasonable power (R^2 values in the range of 0.6–0.7). Since future advances in micro-scale technology providing cheaper and more reliable sensors, the adoption of LCM alternatives to conventional monitoring stations can be expected to grow although not for regulatory purposes.

4. Conclusions

This study demonstrates the use of data obtained with continuously reading LCMs. Although the LCM data are less accurate than scientific-grade instruments, they provide continuous measurements at many locations over a whole season that can be calibrated to provide useful estimates of the concentrations over time and space. This study has limitations. Current LCMs for PM use dust sensors based on light scattering and estimate the PM mass concentration by implementing algorithms developed under lab conditions. Hence, data provided by LCMs will not provide the same accuracy as conventional PM reference methods. Careful instrument calibration and data validation are needed prior to and after the sampling campaigns to ensure unbiased data. In addition, the LCMs do not perform well for low PM concentrations. The LCM technology needs to be improved to better approximate ambient PM concentrations similar to conventional monitoring instruments and efforts are underway to make such improvements. This study supports the use of LCMs with LUR modeling to provide useful estimates of the intraurban spatial and temporal variations of PM at reasonable costs such that this approach can be replicated in other locations where improved exposure assessments are needed.

Acknowledgements

This work was supported by the New York State Energy Research and Development Authority (NYSERDA) under agreement #63040. The authors gratefully acknowledge: (i) Airviz Inc. for the valuable support and maintenance of the Speck monitors used in this study; (ii) the New York State Department of Environmental Conservation for providing the air quality data measured at DEC site as well as allowing us to monitor there; (iii) all the anonymous volunteers who have joined the project; and (iv) Jakub Krček, Stefania Squizzato, and Gursumeeran Satsangi for their help during the sampling campaigns.

Appendix A. Supporting information

Supplementary data associated with this article can be found in the online version at <http://dx.doi.org/10.1016/j.envres.2018.06.052>.

References

- Akbarzadeh, M.A., Khareshi, I., Sharifi, A., Yousefi, N., Naderian, M., Namazi, M.H., Safi, M., Vakili, H., Saadat, H., Alipour Parsa, S., Nickdoost, N., 2018. The association between exposure to air pollutants including PM10, PM2.5, ozone, carbon monoxide, sulfur dioxide, and nitrogen dioxide concentration and the relative risk of developing STEMI: a case-crossover design. *Environ. Res.* 161, 299–303.
- Anderson, J.O., Thundiyil, J.G., Stolbach, A., 2012. Clearing the air: a review of the effects of particulate matter air pollution on human health. *J. Med. Toxicol.* 8 (2), 166–175.
- Argacha, J.F., Collart, P., Wauters, A., Kayaert, P., Lochy, S., Schoors, D., Sonck, J., de Vos, T., Forton, M., Brasseur, O., Beauloye, C., Gevaert, S., Evrard, P., Coppieters, Y., Sinnaeve, P., Claeys, M.J., 2016. Air pollution and ST-elevation myocardial infarction: a case-crossover study of the Belgian STEMI registry 2009–2013. *Int. J. Cardiol.* 223, 300–305.
- Beckerman, B.S., Jerrett, M., Martin, R.V., Van Donkelaar, A., Ross, Z., Burnett, R.T., 2013a. Application of the deletion/substitution/addition algorithm to selecting land-use regression models for interpolating air pollution measurements in California. *Atmos. Environ.* 77, 172–177.
- Beckerman, B.S., Jerrett, M., Serre, M., Martin, R.V., Lee, S.-J., Donkelaar, A., 2013b. A hybrid approach to estimating national scale spatiotemporal variability of PM_{2.5} in the contiguous United States. *Environ. Sci. Technol.* 47 (13), 7233–7241.
- Beelen, R., Voogt, M., Duyzer, J., Zandveld, P., Hoek, G., 2010. Comparison of the performances of land-use regression modelling and dispersion modelling in estimating small-scale variations in long-term air pollution concentrations in a Dutch urban area. *Atmos. Environ.* 44 (36), 4614–4621.
- Budde, M., El Masri, R., Riedel, T., Beigl, M., 2013. Enabling low-cost particulate matter measurement for participatory sensing scenarios. In: Proceedings of the 12th International Conference on Mobile and Ubiquitous Multimedia - MUM '13, 1–10.
- Budde, M., Zhang, L., Beigl, M., 2014. Distributed, low-cost particulate matter sensing: scenarios, challenges, approaches. *ProScience* 2014, 1, In: Proceedings of the First International Conference on Atmospheric Dust - DUST 2014, pp. 230–236.
- Carminati, M., Ferrari, G., Sampietro, M., 2017. Emerging miniaturized technologies for airborne particulate matter pervasive monitoring. *Meas. J. Int. Meas. Confed.* 101, 250–256.
- Clougherty, J.E., Wright, R.J., Baxter, L.K., Levy, J.I., 2008. Land-use regression modeling of intra-urban residential variability in multiple traffic-related air pollutants. *Environ. Heal.* 7 (1), 17.
- Clougherty, J.E., Kheirbek, I., Eisl, H.M., Ross, Z., Pezeshki, G., Gorczynski, J.E., Johnson, S., Markowitz, S., Kass, D., Matte, T., 2013. Intra-urban spatial variability in wintertime street-level concentrations of multiple combustion-related air pollutants: the New York City Community Air Survey (NYCCAS). *J. Expo. Sci. Environ. Epidemiol.* 23 (3), 232–240.
- Covert, D.S., Charlson, R.J., Ahlquist, N.C., 1975. A study of the relationship of chemical composition and humidity to light scattering by aerosols. *J. Appl. Meteorol.* 11, 968–976.
- Dadvand, P., Parker, J., Bell, M.L., Bonzini, M., Brauer, M., Darrow, L.A., Gehring, U., Glinianaia, S.V., Gouveia, N., Ha, E.H., et al., 2013. Maternal exposure to particulate air pollution and term birth weight: a multi-country evaluation of effect and heterogeneity. *Environ. Health Perspect.* 121 (3), 367–373.
- Eeftens, M., Beelen, R., de Hoogh, K., Bellander, T., Cesaroni, G., Cirach, M., Declercq, C., Dedele, A., Dons, E., de Nazelle, A., et al., 2012. Development of land-use regression models for PM_{2.5}, PM_{2.5} 5 absorbance, PM₁₀ and PM_{coarse} in 20 European study areas, results of the ESCAPE project. *Environ. Sci. Technol.* 46 (20), 11195–11205.
- Emami, F., Masiol, M., Hopke, P.K., 2018. Air pollution at Rochester, NY: long-term trends and multivariate analysis of upwind SO₂ source impacts. *Sci. Total Environ.* 612, 1506–1515.
- Gardner, B., Ling, F., Hopke, P.K., Frampton, M.W., Utell, M.J., Zareba, W., et al., 2014. Ambient fine particulate air pollution triggers ST-elevation myocardial infarction, but not non-ST elevation myocardial infarction: a case-crossover study. *Part Fibre Toxicol.* 11, 1. <http://dx.doi.org/10.1186/1743-8977-11-1>.
- Gozzi, F., Della Ventura, G., Marcelli, A., 2016. Mobile monitoring of particulate matter: state of art and perspectives. *Atmos. Pollut. Res.* 7 (2), 228–234.

- Halliburton, B.W., Carras, J.N., Nelson, P.F., Morrison, A.L., Rowland, R., 2007. Comparison of three different real time particle measuring instruments. In Proceedings of the 14th IUAPPA World Congress: Clean Air Partnerships: Coming Together for Clean Air: Brisbane 2007: Conference, incorporating the 18th CASANZ Conference hosted by the Clean Air Society of Australia and New Zealand, Doley, D., Ed., Brisbane, pp. 9–13.
- Hodzic, A., Vautard, R., Bessagnet, B., Lattuati, M., Moreto, F., 2005. Long-term urban aerosol simulation versus routine particulate matter observations. *Atmos. Environ.* 39 (32), 5851–5864.
- Hoek, G., Beelen, R.M.J., de Hoogh, K., Vienneau, D., Gulliver, J., Fischer, P., Briggs, D., 2008. A review of land-use regression models to assess spatial variation of outdoor air pollution. *Atmos. Environ.* 42 (33), 7561–7578.
- Hoek, G., Beelen, R., Kos, G., Dijkema, M., Zee, S.C., Van Der, Fischer, P.H., Brunekreef, B., 2011. Land-use regression model for ultrafine particles in Amsterdam. *Environ. Sci. Technol.* 45, pp. 622–628.
- Hoek, G., Beelen, R., Brunekreef, B., 2015. Land-use regression models for outdoor air pollution. In: Nieuwenhuijsen, M. (Ed.), *Exposure Assessment in Environmental Epidemiology*. Oxford University Press, Oxford, UK, pp. 271–293.
- Holstius, D.M., Pillariseti, A., Smith, K.R., Seto, E., 2014. Field calibrations of a low-cost aerosol sensor at a regulatory monitoring site in California. *Atmos. Meas. Technol.* 7 (4), 1121–1131.
- Hoogh, K., Wang, M., Adam, M., Badaloni, C., Beelen, R., Birk, M., 2013. Development of land-use regression models for particle composition in twenty study areas in Europe. *Environ. Sci. Technol.* 47.
- Isakov, V., Touma, J.S., Khlystov, A., 2007. A method of assessing air toxics concentrations in urban areas using mobile platform measurements. *J. Air Waste Manag. Assoc.* 57 (11), 1286–1295.
- Kelly, K.E., Whitaker, J., Petty, A., Widmer, C., Dybwad, A., Sleeth, D., Martin, R., Butterfield, A., 2017. Ambient and laboratory evaluation of a low-cost particulate matter sensor. *Environ. Pollut.* 221, 491–500.
- Kumar, P., Morawska, L., Martani, C., Biskos, G., Neophytou, M., Di Sabatino, S., Bell, M., Norford, L., Britter, R., 2015. The rise of low-cost sensing for managing air pollution in cities. *Environ. Int.* 75, 199–205.
- Levy, J.I., Hanna, S.R., 2011. Spatial and temporal variability in urban fine particulate matter concentrations. *Environ. Pollut.* 159 (8–9), 2009–2015.
- Li, L., Zheng, Y., Zhang, L., 2014. Demonstration abstract: PiMi air box - A cost-effective sensor for participatory indoor quality monitoring. In: Proceedings of the 13th International Symposium on Information Processing in Sensor Networks (Part of CPS Week), IPSN 2014, pp. 327–328.
- Lin, H., Liu, T., Xiao, J., Zeng, W., Guo, L., Li, X., Xu, Y., Zhang, Y., Chang, J.J., Vaughn, M.G., et al., 2017a. Hourly peak PM_{2.5} concentration associated with increased cardiovascular mortality in Guangzhou, China. *J. Expo. Sci. Environ. Epidemiol.* 27 (3), 333–338.
- Lin, H., Ratnapradipa, K., Wang, X., Zhang, Y., Xu, Y., Yao, Z., Dong, G., Liu, T., Clark, J., Dick, R., et al., 2017b. Hourly peak concentration measuring the PM_{2.5} -mortality association: results from six cities in the Pearl River Delta study. *Atmos. Environ.* 161, 27–33.
- Loomis, D., Grosse, Y., Lauby-Secretan, B., Ghissassi, F., El, Bouvard, V., Benbrahim-Tallaa, L., Guha, N., Baan, R., Mattock, H., Straif, K., 2013. The carcinogenicity of outdoor air pollution. *Lancet Oncol.* 14 (13), 1262–1263.
- Lundgren, D.A., Cooper, D.W., 1969. Effect of humidity on light-scattering methods of measuring particle concentration. *J. Air Pollut. Control Assoc.* 19, 243–247.
- Manikonda, A., Zikova, N., Hopke, P.K., Ferro, A.R., 2016. Laboratory assessment of low-cost PM monitors. *J. Aerosol Sci.* 102, 29–40.
- NYSERDA, 2015. (New York State Energy Research and Development Authority). *Patterns and Trends New York State Energy Profiles: 1999–2013*. Albany, NY, USA, p. 84.
- Özkaynak, H., Baxter, L.K., Dionisio, K.L., Burke, J., 2013. Air pollution exposure prediction approaches used in air pollution epidemiology studies. *J. Expo. Sci. Environ. Epidemiol.* 23 (6), 566–572.
- Pope, C.A., Ezzati, M., Dockery, D.W., 2009. Fine-particulate air pollution and life expectancy in the United States. *N. Engl. J. Med.* 360 (4), 376–386.
- Pope, C.A., Muhlestein, J.B., Anderson, J.L., Cannon, J.B., Hales, N.M., Meredith, K.G., et al., 2015. Short-term exposure to fine particulate matter air pollution is preferentially associated with the risk of ST-segment elevation acute coronary events. *J. Am. Heart Assoc.* 4, e002506.
- Raaschou-Nielsen, O., Andersen, Z.J., Beelen, R., Samoli, E., Stafoggia, M., Weinmayr, G., Hoffmann, B., Fischer, P., Nieuwenhuijsen, M.J., Brunekreef, B., et al., 2013. Air pollution and lung cancer incidence in 17 European cohorts: prospective analyses from the European Study of Cohorts for Air Pollution Effects (ESCAPE). *Lancet Oncol.* 14 (9), 813–822.
- Rich, D.Q., Utell, M.J., Croft, D.P., Thurston, S.W., Thevenet-Morrison, K., Evans, K.A., Ling, F., Tian, Y., Hopke, P.K., 2018. Daily land use regression estimated woodsmoke and traffic pollution concentrations and the triggering of ST-elevation myocardial infarction: a case-crossover study. *Air Qual. Atmos. Health* 11 (2), 239–244. <http://dx.doi.org/10.1007/s11869-017-0537-1>.
- Sarnat, S.E., Klein, M., Sarnat, J.A., Flanders, W.D., Waller, L.A., Mulholland, J.A., Russell, A.G., Tolbert, P.E., 2010. An examination of exposure measurement error from air pollutant spatial variability in time-series studies. *J. Expo. Sci. Environ. Epidemiol.* 20 (2), 135–146.
- Shairsingh, K.K., Jeong, C.H., Wang, J.M., Evans, G., 2018. Characterizing the spatial variability of local and background concentration signals for air pollution at the neighbourhood scale. *Atmos. Environ.* 183, 57–68.
- Sinisi, S.E., van der Laan, M.J., 2004a. Deletion/substitution/addition algorithm in learning with applications in genomics. *Stat. Appl. Genet. Mol. Biol.* 3 (1), Article18.
- Sinisi, S.E., van der Laan, M.J., 2004b. Loss-based cross-validated deletion/substitution/addition algorithms in estimation. U.C. Berkeley Div. Biostat. Work. Pap., Working Paper.
- Snyder, E.G., Watkins, T.H., Solomon, P.A., Thoma, E.D., Williams, R.W., Hagler, G.S.W., Shelow, D., Hindin, D.A., Kilaru, V.J., Preuss, P.W., 2013. The changing paradigm of air pollution monitoring. *Environ. Sci. Technol.* 47, 11369–11377.
- Solomon, P.A., Crumpler, D., Flanagan, J.B., Jayanty, R.K.M., Rickman, E.E., McDade, C.E., 2014. U.S. national PM_{2.5} chemical speciation monitoring networks-CSN and IMPROVE: description of networks. *J. Air Waste Manag. Assoc.* 64 (12), 1410–1438.
- Sousan, S., Koehler, K., Thomas, G., Park, J.H., Hillman, M., Halterman, A., Peters, T.M., 2016. Inter-comparison of low-cost sensors for measuring the mass concentration of occupational aerosols. *Aerosol Sci. Technol.* 50 (5), 462–473.
- Su, J.G., Hopke, P.K., Tian, Y., Baldwin, N., Thurston, S.W., Evans, K., Rich, D.Q., 2015a. Modeling particulate matter concentrations measured through mobile monitoring in a deletion/substitution/addition approach. *Atmos. Environ.* 122, 477–483.
- Su, J.G., Jerrett, M., Meng, Y.Y., Pickett, M., Ritz, B., 2015b. Integrating smart-phone based momentary location tracking with fixed site air quality monitoring for personal exposure assessment. *Sci. Total Environ.* 506–507, 518–526.
- Thurston, G.D., Roberts, E.M., Ito, K., Pope III, C.A., Glenn, B.S., Ozkaynak, H., Utell, M.J., Bekkedal, M.Y.V., 2009. Use of health information in air pollution health research: past successes and emerging needs. *J. Expo. Sci. Environ. Epidemiol.* 19, 45–58.
- Turner, J.R., Hansen, A.D., Allen, G.A., 2007. Methodologies to Compensate for Optical Saturation and Scattering in Aethalometer TM Black Carbon Measurements. In: Proceedings from the Symposium on Air Quality Measurement Methods and Technology, San Francisco, CA, USA.
- US EPA, 2017. Evaluation of Emerging Air Pollution Sensor Performance. (<https://www.epa.gov/air-sensor-toolbox/evaluation-emerging-air-pollution-sensor-performance>) (accessed Nov 1, 2017).
- Virkkula, A., Mäkelä, T., Hillamo, R., Yli-Tuomi, T., Hirsikko, A., Hämeri, K., Koponen, I.K., 2007. A simple procedure for correcting loading effects of aethalometer data. *J. Air Waste Manag. Assoc.* 57 (10), 1214–1222.
- Wang, Y., Hopke, P.K., Rattigan, O.V., Xia, X., Chalupa, D.C., Utell, M.J., 2011. Characterization of residential wood combustion particles using the two-wavelength aethalometer. *Environ. Sci. Technol.* 45 (17), 7387–7393.
- Wang, Y., Hopke, P.K., Xia, X., Chalupa, D.C., Utell, M.J., 2012. Source apportionment of airborne particulate matter using inorganic and organic species as tracers. *Atmos. Environ.* 55, 525–532.
- Wang, Y., Li, J., Jing, H., Zhang, Q., Jiang, J., Biswas, P., 2015. Laboratory evaluation and calibration of three low-cost particle sensors for particulate matter measurement. *Aerosol Sci. Technol.* 49, 1063–1077.
- Zhang, M.Q., Qi, W., Yao, W., Wang, M., Chen, Y., Zhou, Y., 2016. Ambient particulate matter (PM_{2.5}/PM₁₀) exposure and emergency department visits for acute myocardial infarction in Chaoyang District, Beijing, China during 2014: a case-crossover study. *J. Epidemiol.* 26, 538–545.
- Zikova, N., Hopke, P.K., Ferro, A.R., 2017a. Evaluation of new low-cost particle monitors for PM_{2.5} concentrations measurements. *J. Aerosol Sci.* 105, 24–34.
- Zikova, N., Masiol, M., Chalupa, D.C., Rich, D.Q., Ferro, A.R., Hopke, P.K., 2017b. Estimating hourly concentrations of PM_{2.5} across a metropolitan area using low-cost particle monitors. *Sensors* 17 (8).